ARCHIVES OF ELECTRICAL ENGINEERING VOL. 70(4), pp. 845–858 (2021)

DOI 10.24425/aee.2021.138265

Low altitude control for quadcopter using visual feedback

KONRAD URBANSKI

Institute of Robotics and Machine Intelligence
Poznan University of Technology
Piotrowo 3A str., 60-965 Poznan, Poland
e-mail: konrad.urbanski@put.poznan.pl

(Received: 17.12.2020, revised: 09.05.2021)

Abstract: The paper presents the results of simulations and experiments in the field of control of the low damping and time delay oscillating system. This system includes a quadcopter hovering at a very low altitude, and the altitude is controlled. The time delay is introduced mainly by the remote control device. In order to handle the quadcopter at low altitudes, a proportional-integral controller with a negative proportional coefficient is used. Such an approach can provide good results in the case of an oscillating, low damped system. This method of steering, which uses a typical radio control transmitter, can be used on any commercially available leisure drone. Feedback is provided by a camera and algorithms of computer vision. The presented results were obtained experimentally using free flight – without a harness. Different types of controllers are used to control horizontal shift and altitude.

Key words: control, estimation, ground effect, visual servoing

1. Introduction

In recent years, there has been a rapid increase in the interest in unmanned aerial vehicles (UAVs). The reason is the lower cost of advanced electronic systems, as well as UAV equipment with sensors and algorithms to facilitate piloting. This research aims to develop algorithms for the control for a quadcopter position control system for a specific control axis – in this case, the altitude. For altitude-axis control purposes in a very low altitude range, the plant can be simplified to a non-linear oscillating object with low damping with time delay. The system includes a quadcopter and its control electronics, including a remote control transmitter. Although

control methods for oscillating objects are known, especially in the case of linear objects, they relate to objects with parameters significantly different from these (small) drones and apply to objects, analysed in terms of sensitivity to a completely different type or range of disturbances. Such typical oscillatory objects known from the literature are, for example, trains, trucks, gantries, and cranes [1–3]. The issue of altitude control in the field of low altitude is particularly important due to the strong impact of the ground effect and disturbances caused by air turbulence caused by obstacles and the influence of air currents. The described disturbances have a significant impact on drones of low weight (under one kilogram), which are highly susceptible to external disturbances. Such conditions may occur, for example, when exploring ducts and interior or other tight spaces in the immediate vicinity of obstacles. The presented master control system for the quadcopter position control works as follows: it recognises the location of the quadcopter on the frame of the camera image (the camera is directed towards the drone) and then correctly controls the throttle and the roll. The results presented in this article concern low altitude flights. The impact range of the ground effect is determined in the range of about 3 to 5 multiples of the rotor radius [4–6]. The research of multicopters' control systems is still a current research task. The use of visual feedback can be a way to avoid altitude determination with the use of a barometric sensor, which may be inaccurate [7]. The way of the autonomous landing using the infrared marker is presented in [8]. Visual feedback may be used in many different ways: in [9], the onboard camera is used in order to control the position during hovering. Visual feedback is also used for drive control and robot motion control [10, 11]. The use of tracking algorithms to control a rotorcraft is presented in [12], and a method combining foreground detection and online feature classification in order to detect UAVs visually is presented in [13].

This article presents an unusual approach to determining the structure of the altitude controller for a quadcopter flying in the range of the ground effect. In the present article, a novelty is an approach that allows modelling a multicopter located in the ground effect impact range as an oscillating object (instead of a double-integrating one). Such an approach allows for the analytical selection of the parameters of the controller working in this altitude range. Good control properties were obtained by using the negative proportional part of the IP controller, which is not common in the bibliography. A Viola–Jones detector was used to determine the location of the quadcopter. The captured frames from the video stream generated by the camera are analysed in real-time. Then, the appropriate procedures analyse the results of the detector operation by rejecting false matches.

2. Viola–Jones multicopter detector

The location of the object is based on Haar-like classifiers [14], which determines the set of possible quadcopter locations in the captured frame and then outputs its coordinates. Before using such a detector, however, the following steps should be taken: using the *opencv* library built-in tools, the training procedure should be started using the *opencv_traincascade* application. After successfully defining the detector (this is done once, *off-line*), the control loop starts. The captured frame is converted to grayscale. Then, a process of object detection in the input image is performed. The detected objects are returned as a list. Then, images considered as *false positive* are rejected. Images recognised as *true positive* and *false negative* are processed further. All altitude indications

provided are obtained using the classifiers prepared in the manner described. There is no real altitude measurement, as only its estimation is implemented (except for the simulation). The detailed classifier preparing procedure is described in [15].

3. The control algorithms

The commonly considered control structures in the case of the multicopter are PD (Proportional–Derivative) controllers [16,17] (in general – for attitude control) and PID (Proportional–Integral–Derivative) controllers [18,19] also fractional order controllers [20,21]. Other control structures used in the UAV are SM (Sliding Mode) or enhanced version of SM [22], or MRAC (Model Reference Adaptive Controller) [23]. Controllers based on ANN (Artificial Neural Network) and their combination with PID are also used [24,25]. By analysing the step response results, it was assumed that in the range of noticeable impact of the ground effect, the studied quadcopter's step response looks like the response of an oscillating object with low damping and time delay. Therefore, the following types of controllers were considered in this study for Y-axis control: an integrating-only controller (I), PI (Proportional–Integral) controller with a negative proportional coefficient [26] (marked as "–PI") and 2DOF (Two Degree of Freedom) controller at IP topology, also with a negative proportional coefficient (marked as "IP–").

This is a topology known as the *feedback type 2DOF* (Fig. 1). Saturation block corresponds to a range of throttle control. The PI type controller with all positive coefficients has not worked properly in this application. In the presented approach, as a first control structure, the integrating only controller was used. Such a simple controller (only one degree of freedom) is easy to tune and was used as a reference controller for the altitude.

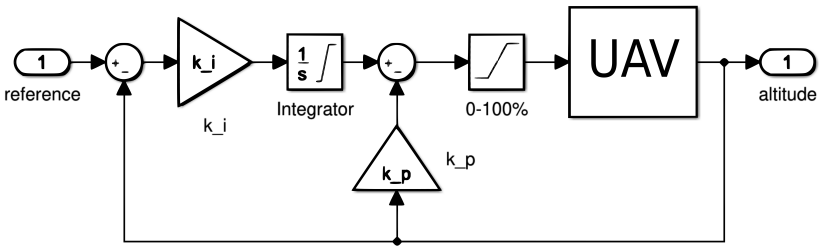

Fig. 1. Diagram of considered control system

Simulations have shown, however, that –PI and IP– are characterised by the best damping.

A PD controller was used for the control algorithm for horizontal shift (X-axis). The controller was set using its own optimisation algorithm on a real object (algorithm adopted from [27] – a "full" mode). This algorithm starts and stops manually. The function is written in *Python 3* as part of the control and development algorithm. At this stage of investigations, the PD controller gives the best results in the X-axis. The improvement and analysis of controlling the X-axis is the subject of future work. A general view of the control system is shown in Fig. 2.

In this figure, the rounded rectangles indicate the software. The control algorithms and the position estimation are fulfilled using *Python* and *opencv* libraries. It should be mentioned that

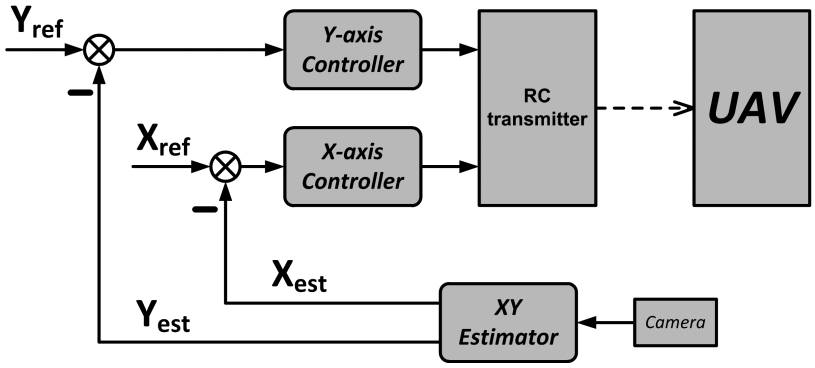

Fig. 2. General scheme with the 2DOF controller used in the altitude axis

the algorithms presented in the literature use much higher ranges of calculation loop frequencies: 30 Hz, 100 Hz, 200 Hz or even 400 Hz. In the scope of realised experiments, the presented system uses an external control loop with a frequency of 10 Hz, which is much lower than usually used. However, good results were obtained.

4. Modelling the low altitude control loop

Maintaining the reference altitude in the case of a small (light) quadcopter is hard, especially in the case of the relatively long calculation period of the controller compared to the UAV's time constants. In addition, a time delay has been identified in the control loop. It is clearly seen that such an object is hard to control, especially in the presence of time-varying disturbances. Dealing with the ground effect forces the change of control strategy from "typical" (using a dual integrating model of quadcopter) to a new control strategy, suitable for this low altitude range. This can be particularly important when manoeuvring at low altitude. At this stage of the research, the ground effect was included in the model by changing its parameters. It was assumed that no internal data of the quadcopter's state (attitude, speed, acceleration) are available. This means that the control algorithm can only use an estimated position through a detector.

This is the reason for using a simple model of the controlled object. Firstly, an object was identified using the open-loop step response (Fig. 3). The reference throttle was changed from 28% to 36% (at about 25% throttle, the copter starts hovering). It is noticeable that this response looks similar to a second-order under-damped system with time delay ($\tau = 0.5$ s). It is also visible that the oscillation period is changing. It was assumed that this depends on the actual altitude. As a result of this observation, a simple model of the quadcopter in the Y-axis was proposed. It was assumed that this step response can be approximated by a second-order system plus dead time with a variable oscillation period, complemented by gravitational force:

$$T^2(h)\frac{\mathrm{d}^2h}{\mathrm{d}t^2} + 2\zeta T(h)\frac{\mathrm{d}h}{\mathrm{d}t} + h = K\left(F_{\mathrm{thr}}(t-\tau) - mg\right), \tag{1}$$

where: K is the gain, F_{thr} is the thrust generated by rotating propellers, τ is the dead time, $T(h)$ is the variable time parameter, ζ is the damping factor, h is the altitude of the quadcopter, g is the acceleration due to gravity, and m is the mass of the UAV.

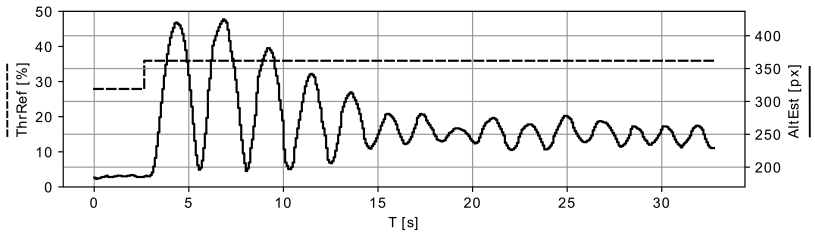

Fig. 3. Experiment: step change of the throttle 28%→36%; *ThrRef* is the reference throttle in [%], *AltEst* is the altitude in [px] (pixel in actual camera view)

In the first approach, the gain K, and the damping factor ζ were also variable, but this did not cause any significant difference in the model's performance in the range of the ground effect impact, compared to the constant average value of K and the damping factor. The air cushion effect allows the modelling of the quadcopter in the Y-axis as a second-order system. This should be smoothly transformed into a double integral with increasing altitude above the influence of the ground effect. For the tested quadcopter, the altitude where changing behaviour from the oscillating system into the double integral began was about 1.2–1.8 m. The next step is determining the controller parameters. Before finding these parameters, however, the control loop elements were specified. An altitude controller outputs reference throttle value in the range of 0–100% in the analysed case. The thrust is calculated using a well-known simplified relationship:

$$F_{\text{thr}} = k_{\text{thr}} \cdot (\omega_{\text{ref}})^2 , \tag{2}$$

where k_{thr} is the gain and ω_{ref} is the average reference speed of rotors.

Assuming that the altitude controller calculation period is significantly longer than the time constant of the inner motor speed control path, ω_{ref} is calculated from the simplified relationship:

$$\omega_{\text{ref}} = k_1 \cdot (u_{\text{ctrl}})^{k_2} , \tag{3}$$

where k_1 and k_2 are the gains and u_{ctrl} is the control signal generated by the altitude controller (throttle). Equations (2) and (3) can be simplified:

$$F_{\text{thr}} = k_{F1} \cdot (u_{\text{ctrl}})^{k_{F2}} , \tag{4}$$

where k_{F1} and k_{F2} are the "new" gains.

The gains from (1), (4) and the value of ζ were chosen using the optimisation (identification) procedure performed in *Matlab* and the recorded data for the closed-loop step response. This test was performed for the integrating type of controller in the case of the absence of any external disturbances. The relationship $T(h)$ is fulfilled as the lookup table. Its nodes are determined through measurements of the open-loop step response waveform (Fig. 3), as well as the dead time value τ. Based on this model, it is possible to find the controller structure for altitude control. Using

Matlab's *optimtool* for three selected control structures: I, PI, and IP, the optimisation procedure was initiated. The *fminsearch* method and IAE (Integral Absolute Error) quality function were chosen as a solver. It was assumed that in the ground effect impact range, the controller's parameters are constant. The test run for the parameter selection process is shown in Fig. 4(a).

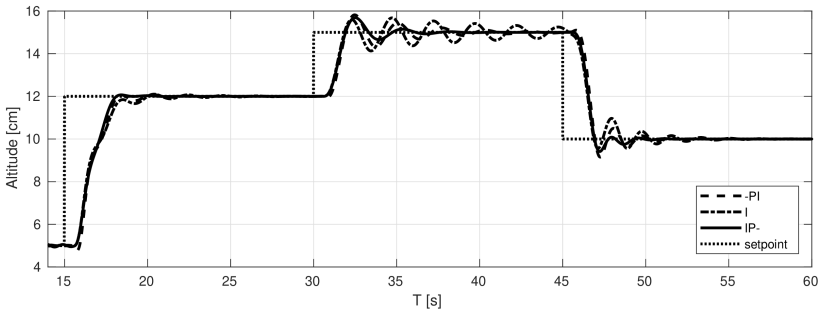

(a)

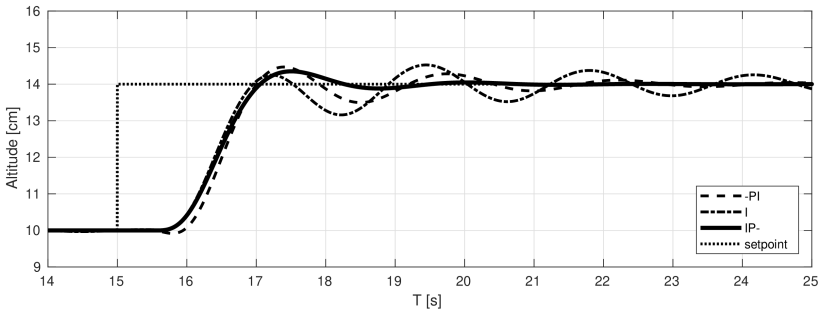

(b)

Fig. 4. Simulation – step responses for optimised controller parameters (non-linear model): (a) setpoint change sequence for optimisation; (b) example step response

It can be seen that with constant controller parameters, the quality of control depends on the flight altitude. In addition, in the case of proportional–integral controllers, a negative proportional factor coefficient was selected during optimisation (both for PI and IP structures) for both structures. Tests have shown that in this case, structure IP– suppresses oscillations faster (Fig. 4(b)) and has a better-quality index than structure –PI (Table 1).

Table 1. Parameters corresponding to the waveforms from Fig. 4(a)

Structure	**Quality index IAE**	k_p	k_i
I	148	0.0	0.1
–PI	142	–0.012	0.1
IP–	125	–0.024	0.093

In addition, it is visible that the –PI step response is quite similar to the step response of a non-minimum phase linear system (Fig. 4(b), at $T = 16$ s). So, the IP– controller structure was selected for further experimental testing. The positive impact of a negative proportional factor coefficient can be confirmed from the other side by analysing the open-loop system. A linearised model of the object described by (1) and (4) was made (the feedback path transfer function is equal to 5 in this model):

$$G_O(s) = \frac{1.2e^{-0.5s}}{0.09s^2 + 0.026s + 1}. \tag{5}$$

Figure 5 shows the results of changing the sign k_p and switching off the proportional unit ($k_p = 0$) of the controller. It can be seen that in the case of a negative k_p coefficient (with an appropriate value) or zero, the path is on the right of the critical point (–1, j0). The controller parameters determined by simulation were implemented after scaling in a real system. In the case of results presented in Fig. 8, they only required minor modifications to the IP– controller to improve performance: from {0.093, –0.024} to {0.1, –0.015}. The best performance with an integrating-only controller was achieved without parameter adjustment ($k_i = 0.1$).

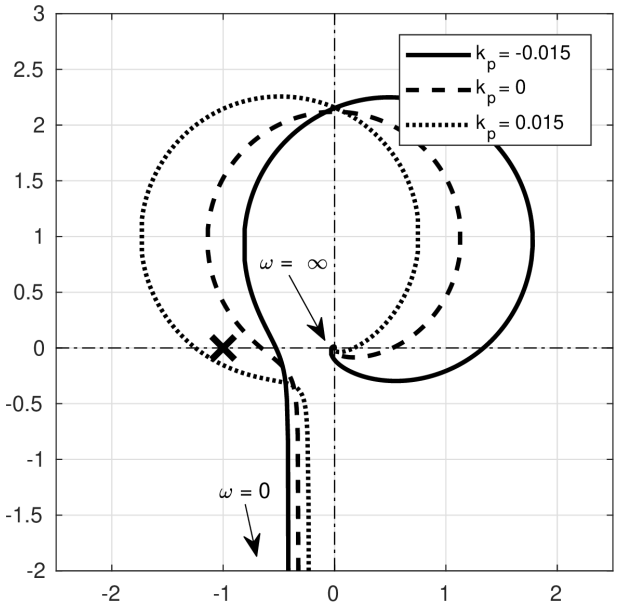

Fig. 5. The Nyquist plot for {–PI, I, PI} controller and linearized plant model (5)

5. The experimental setup

Experimental studies are carried out using commercially available components. As a result, upon developing software that uses standard communication protocols, the system is ready for operation. Every component is ready to use, and there is no need for cumbersome starting procedures. This approach provides the opportunity to focus on the main task: external loop control

algorithms for position control, enabling quick reconfiguration from one commercial device to another. The condition of using a given device is the presence of the external control mode in the wireless transmitter. Originally, it was prepared for training with connected transmitters, one for the trainer and one for the trainee. This mode, however, can also be used for UAV control by a computer without the need for hardware modifications. The presented system consists of a camera, personal computer (managed by *Ubuntu*, an open-source operating system), USB → PPM (Pulse Position Modulation) interface, transmitter, and controlled object – a commercially available quadcopter: weight: 147 g (including battery), supply: 2 S 850 mA·h Li-Po battery, dimensions: $16 \times 16 \times 5$ [cm] (without antennas). Rotor radius: 3.5 cm. The multicopter used in the experiments is shown in Fig. 6. The concept of the control system is shown in Fig. 7. The tests were conducted indoors. The room was not sealed. In the room, there were large pieces of equipment (lockers, desks, etc.) within a range of less than 1 m, further interfering with the UAV-induced airflow.

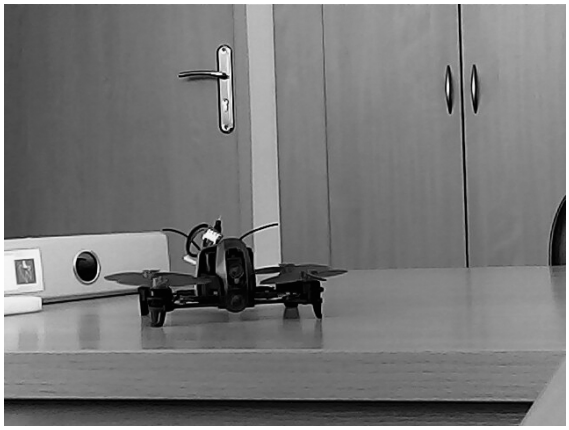

Fig. 6. The multicopter used in experiment

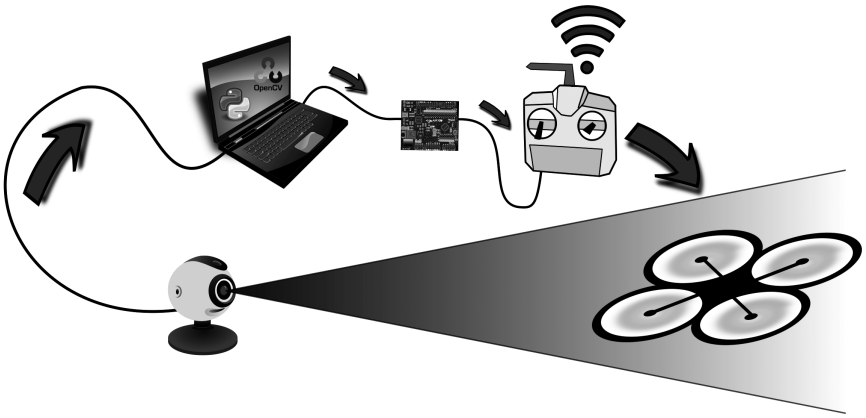

Fig. 7. General view of the hardware configuration used in the experiment

6. Results

The quadcopter detector prepared using the learning procedure was tested while moving the quadcopter. The tests have shown that the quality of the camera used is sufficient to generate an image of a quality suitable for proper processing by the detector. However, the 33 ms–125 ms controller period (set by the camera's hardware) is a boundary value in the context of comparable values of the mechanical time constant (500 ms of dead time and average second-order time constant about 300 ms) of the UAV. This has a considerable impact on the quality of control. The identified damping factor is equal to $\zeta = 0.04$.

The tests were carried out regarding the functionality of visual feedback in terms of quadcopter position control using the closed-loop system, i.e., when the estimated position is used in the control path. The tests were carried out indoors, in the presence of random disturbances (in the form of breeze) and a short distance from obstacles such as chairs, shelves etc. (which causes significant air turbulence). Figure 8 shows the waveforms for hovering tests. The upper waveforms represent the fixed reference altitude (*AltRef*) and the estimated altitude (*AltEst*) in [px] (frame pixels). Reference altitude was set to 11 cm. Different values in pixels for the same setpoint are caused by (minor) differences in camera position. This is not important for the control concept because the assumption is to control the position selected in the visible frame (at this stage of research, it is the X and Y positions in the camera frame) for the current camera attitude. The middle waveforms represent the fixed horizontal shift position (*PosRefX*) and the estimated horizontal position (*PostEstX*), also in [px]. This reference position was set in the middle of

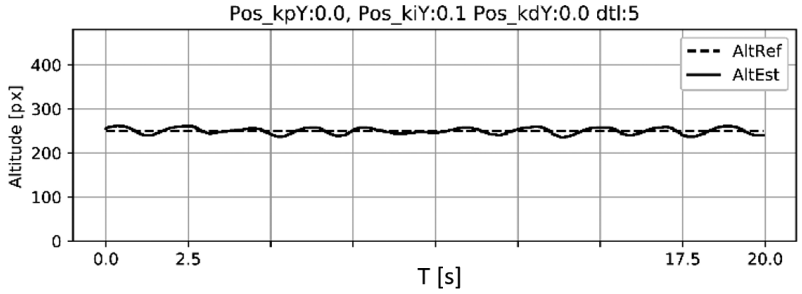

(a)

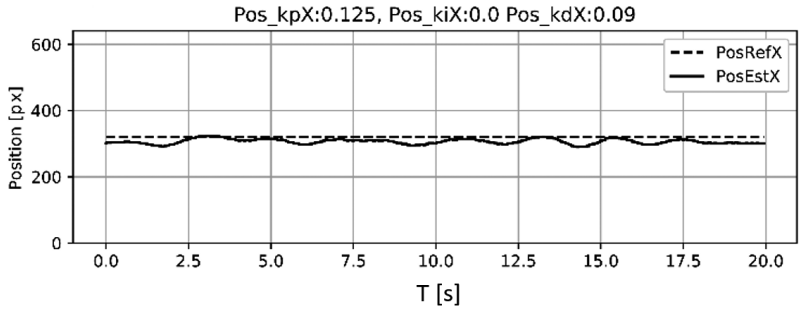

(b)

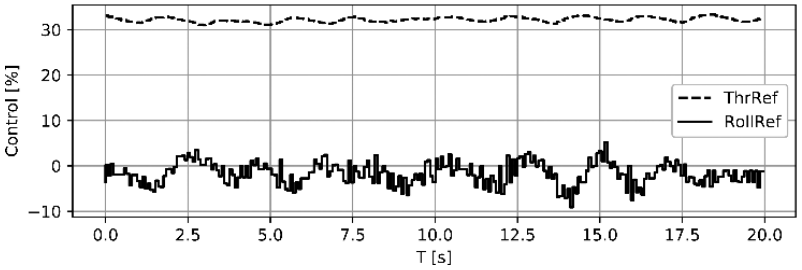

(c)

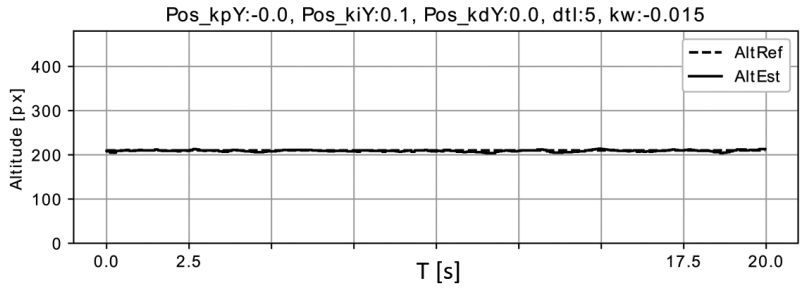

(d)

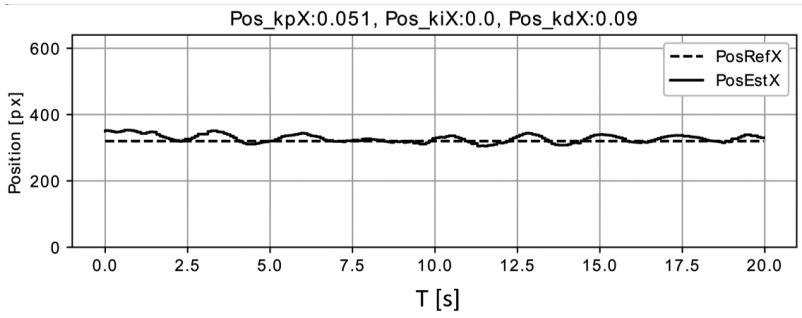

(e)

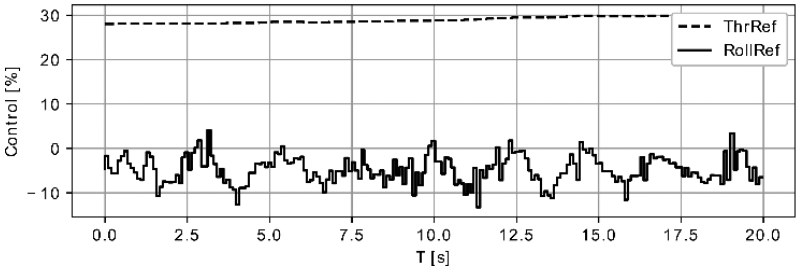

(f)

Fig. 8. Experiment, hovering, altitude about 11 cm: (a)–(c) I-type altitude controller, IAE = 122; (d)–(f) IP–altitude controller, IAE = 33

a frame. As mentioned before, the control of the X-axis is not yet optimised; however, the control-related waveforms in this axis are presented to show their correct operation. For both axes (X and Y) – altitude and horizontal shift – no interaction is visible. The *dtl* "filter" variable visible in Fig. 8 denotes the number of samples from which the mean value for the position of the output vector was calculated. The waveforms in Fig. 8(c) and Fig. 8(f) represent the reference throttle (*ThrRef*) and the reference roll (*RollRef*) in [%]. The scale of the X and Y axes was chosen so that the entire range visible to the camera is shown. Sampling: about 100 ms (imposed by the camera, usually dark conditions); resolution of the feedback signal: one pixel from 640×480; control signal resolution: $1/1000$. The system was tested at a distance of approximately 0.5 m to 3 m (for indoor experiments). The quadcopter was correctly recognised in sizes (bounding boxes) from 40×20 [px] to 100×50 [px] and even larger. In the case of small sizes, the detector was switched to another one, learned on small objects. Figs. 8(a)–8(c) show the test results for the integrating-only type of altitude controller. Such a controller is easy to tune; however, it has limited performance. After all, the desired altitude is maintained. The perturbations decay slowly – oscillations are permanently visible (Fig. 8(a)). The integrating controller does not provide a fast response to the rapid change of error value. In the case of minor disruptions in the X-axis, the PD horizontal shift controller reliably holds the position reference value. Figures 8(d)–8(f) show the system's operation for an IP– type altitude controller, and with an X-axis controller also implemented as a PD structure. The desired altitude is maintained with satisfactory quality. Perturbations decay fast (Fig. 8(d). The process of optimising the controller parameters during the experiment confirmed the higher efficiency of the IP controller with a negative proportional factor. There is a clear difference in performance quality based on the IAE value obtained for the period shown. Finally, in Fig. 9, the results of the operation of the control loop are shown in

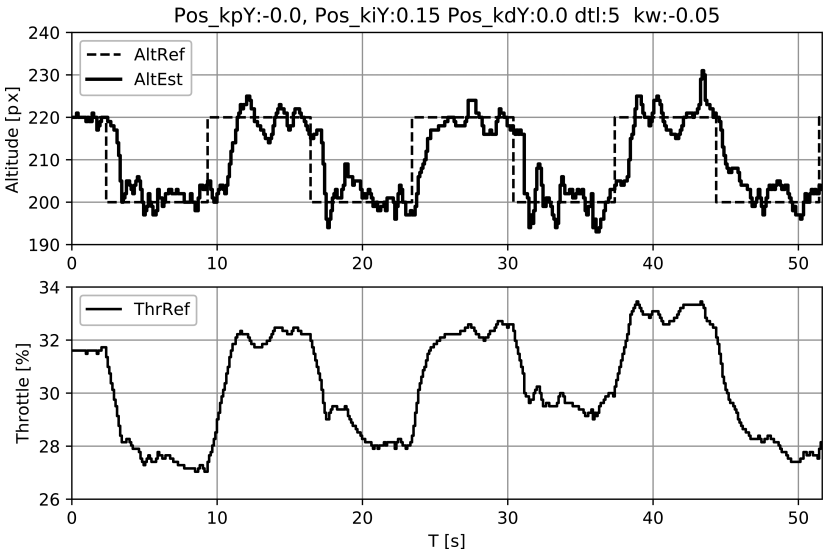

Fig. 9. Experiment: IP–altitude controller. Operation of the control algorithm (closed loop), reference altitude step from about 6 cm (200 px) to about 16 cm (220 px); up: referenced (*AltRef*) and estimated (*AltEst*) altitude, raw (not filtered) data; down: control signal of the reference throttle

the case of a sequence of a step-change in reference altitude from 6 cm to 16 cm. The influence of interference (air currents) is visible in the estimated altitude. The controller, however, allows maintaining the desired altitude for both the upper and lower values. The current camera position corresponds to the values of 200 pixels and 220 pixels. It should be noted that the tests, although indoors, were carried out in real conditions, where the UAV was exposed to the continuous impact of disturbances of changing values and directions.

7. Conclusions

This paper presents an idea of approximation for a quadcopter model at a low altitude as a second-order underdamped system. It makes it possible that the controller structure and settings can be analytically determined for this altitude range. In order to control the quadcopter in the Y-axis, different types of controllers were checked. Altitude was controlled using an integrating or proportional-integral structure with a *negative proportional coefficient*. The negative proportional component improves maintaining the set altitude in this low altitude range by avoiding the excitation of oscillations and their amplification. A non-linear quadrocopter model was proposed for the Y axis, allowing the controller structure selection by simulation. The model and control method are valid in the range of ground effect impact. It is possible to control the drone's position in one plane without complex high-speed multiple camera laboratory equipment. A Viola–Jones detector makes it possible to control a dynamic object in a closed-loop system. The experiment proves that a simple proportional-integral controller with appropriately selected parameters enables correct altitude maintenance at low altitudes within the specified range. This is a particularly good result, considering the following:

- Low operating frequency (10 Hz on average) for an altitude loop, in contrast to the frequency up to 200 Hz presented in the literature.
- Time delay $\tau = 0.5$ s in a control loop. This value is in the same order of magnitude as the plant time constant.
- Low weight (below 150 g) affecting susceptibility to even a weak breeze.
- The drone is not equipped with markers, either active or passive.
- It is a toy/leisure drone, not a specialised laboratory device.
- Using only the visual signal for the outer control loop, without using internal quadcopter sensors. It was assumed that the system uses only the data available for the human (drone pilot).

The experiment shows that fast-moving objects can be controlled by means of visual feedback. The drone is correctly detected despite the fact that no special markers are placed on the drone. It works not only in the conditions of an "optically" sterile laboratory. This method of identifying the presence of a quadcopter has been shown to work well, even in the case of a heterogeneous background. The main application of this kind of feedback is programmed flights in places where reflective or barometric sensors or GPS do not work correctly, e.g., in narrow or cluttered spaces or underground. The presented visual feedback system could also be used in anti-drone systems in which the interceptor drone detects, recognises and autonomously directs itself at the detected unit.

Future work will include improving the quality of control by increasing the working frequency of the external loop by using a camera with a higher frame rate. It is also planned to use a more advanced controller structure. A detailed analysis of the selection of the structure and parameters of the X-axis controller will also be carried out.

Acknowledgements

This research was supported in part by PL-Grid Infrastructure [28].

References

[1] Hu Y., Wu B., Vaughan J., Singhose W., *Oscillation suppressing for an energy efficient bridge crane using input shaping*, 9th Asian Control Conference (ASCC), IEEE, pp. 1–5 (2013), DOI: 10.1109/ASCC.2013.6606196.

[2] Watanabe K., Yoshikawa M., Ishikawa J., *Damping control of suspended load for truck cranes in consideration of second bending mode oscillation*, in IECON 2018 – 44th Annual Conference of the IEEE Industrial Electronics Society, IEEE, pp. 4561–4568 (2018), DOI: 10.1109/IECON.2018.8591232.

[3] Nowicki M., Respondek W., Piasek J., Kozłowski K., *Geometry and flatness of m-crane systems*, Bulletin of the Polish Academy of Sciences: Technical Sciences, vol. 67, no. 5, pp. 893–903 (2019), DOI: 10.24425/BPASTS.2019.130872.

[4] Cheeseman I., Bennett W., *The Effect of the Ground on a Helicopter Rotor in Forward Flight*, Ministry of Supply, Aeronautical Research Council, Reports and Memoranda, A.R.C. Technical Report R.&M., no. 3021 (1957).

[5] Sharf I., Nahon M., Harmat A., Khan W., Michini M., Speal N., Trentini M., Tsadok T., Wang T., *Ground effect experiments and model validation with Draganflyer x8 rotorcraft*, in 2014 International Conference on Unmanned Aircraft Systems (ICUAS), pp. 1158–1166 (2014), DOI: 10.1109/ICUAS.2014.6842370.

[6] Kan X., Thomas J., Teng H., Tanner H.G., Kumar V., Karydis K., *Analysis of Ground Effect for Small-Scale UAVs in Forward Flight*, IEEE Robotics and Automation Letters, vol. 4, no. 4, pp. 3860–3867 (2019), DOI: 10.1109/LRA.2019.2929993.

[7] Xuan-Mung N., Hong S.-K., *Barometric Altitude Measurement Fault Diagnosis for the Improvement of Quadcopter Altitude Control*, 19th International Conference on Control, Automation and Systems (ICCAS), Jeju, Korea (South), pp. 1359–1364 (2019), DOI: 10.23919/ICCAS47443.2019.8971729.

[8] Xuan-Mung N., Hong S.-K., Nguyen N.P., Le Nhu Ngu Thanh Ha, Le T.L., *Autonomous Quadcopter Precision Landing Onto a Heaving Platform: New Method and Experiment*, IEEE Access, vol. 8, pp. 167192–167202 (2020), DOI: 10.1109/ACCESS.2020.3022881.

[9] Xian B., Liu Y., Zhang X., Cao M., Wang F., *Hovering control of a nano quadrotor unmanned aerial vehicle using optical flow*, in Proceedings of the 33rd Chinese Control Conference 2014, pp. 8259–8264 (2014), DOI: 10.1109/ChiCC.2014.6896384.

[10] Scerri J., Djordjevic G.S., Todorovic D., *Modeling and control of a reaction wheel pendulum with visual feedback*, in 2017 International Conference on Control, Automation and Diagnosis (ICCAD), pp. 024–029 (2017), DOI: 10.1109/CADIAG.2017.8075625.

[11] Ito K., Yamakawa Y., Ishikawa M., *Winding manipulator based on high-speed visual feedback control*, in 2017 IEEE Conference on Control Technology and Applications (CCTA), pp. 474–480 (2017), DOI: 10.1109/CCTA.2017.8062507.

[12] Cheng H., Lin L., Zheng Z., Guan Y., Liu Z., *An autonomous vision-based target tracking system for rotorcraft unmanned aerial vehicles*, in 2017 IEEE/RSJ International Conference on Intelligent Robots and Systems (IROS), pp. 1732–1738 (2017), DOI: 10.1109/IROS.2017.8205986.

[13] Dong Q., Zou Q., *Visual UAV detection method with online feature classification*, in 2017 IEEE 2nd Information Technology, Networking, Electronic and Automation Control Conference (ITNEC), pp. 429–432 (2017), DOI: 10.1109/ITNEC.2017.8284767.

[14] Viola P., Jones M., *Rapid object detection using a boosted cascade of simple features*, in Proceedings of the 2001 IEEE Computer Society Conference on Computer Vision and Pattern Recognition, CVPR 2001, vol. 1, pp. I.511–I.518 (2001), DOI: 10.1109/CVPR.2001.990517.

[15] Urbanski K., *Visual Feedback for Control using Haar-Like Classifier to Identify the Quadcopter Position*, in International Conference on Methods and Models in Automation and Robotics MMAR (2018), DOI: 10.1109/MMAR.2018.8485886.

[16] Bouabdallah S., Siegwart R., *Backstepping and Sliding-mode Techniques Applied to an Indoor Micro Quadrotor*, in Proceedings of the 2005 IEEE International Conference on Robotics and Automation, Barcelona, Spain, pp. 2247–2252 (2005), DOI: 10.1109/ROBOT.2005.1570447.

[17] Dikmen I.C., Arisoy A., Temeltas H., *Attitude control of a quadrotor*, in 2009 4th International Conference on Recent Advances in Space Technologies, pp. 722–727 (2009), DOI: 10.1109/RAST.2009.5158286.

[18] Astudillo A., Muñoz P., Álvarez F., Rosero E., *Altitude and attitude cascade controller for a smartphone-based quadcopter*, in 2017 International Conference on Unmanned Aircraft Systems (ICUAS), pp. 1447–1454 (2017), DOI: 10.1109/ICUAS.2017.7991400.

[19] Giernacki W., *Iterative Learning Method for In-Flight Auto-Tuning of UAV Controllers Based on Basic Sensory Information*, Applied Sciences, vol. 9, no. 4, p. 648 (2019), DOI: 10.3390/app9040648.

[20] Shang B., Liu J., Zhang Y., Wu C., Chen Y., *Fractional-order flight control of quadrotor UAS on vision-based precision hovering with larger sampling period*, Nonlinear Dynamics, vol. 97, no. 2, pp. 1735–1746 (2019), DOI: 10.1007/s11071-019-05103-5.

[21] Sadalla T., Horla D., Giernacki W., Kozierski P., *Influence of time delay on fractional-order PI-controlled system for a second-order oscillatory plant model with time delay*, Archives of Electrical Engineering, vol. 66, no. 4, pp. 693–704 (2017), DOI: 10.1515/aee-2017-0052.

[22] Gonzalez-Hernandez I., Salazar S., Lopez R., Lozano R., *Altitude control improvement for a Quadrotor UAV using integral action in a sliding-mode controller*, in 2016 International Conference on Unmanned Aircraft Systems (ICUAS), pp. 711–716 (2016), DOI: 10.1109/ICUAS.2016.7502674.

[23] Wei P., Chan S.N., Lee S., Kong Z., *Mitigating ground effect on mini quadcopters with model reference adaptive control*, International Journal of Intelligent Robotics and Applications, vol. 3, no. 3, pp. 283–297 (2019), DOI: 10.1007/s41315-019-00098-z.

[24] Lopez-Franco C., Gomez-Avila J., Alanis A.Y., Arana-Daniel N., Villaseñor C., *Visual Servoing for an Autonomous Hexarotor Using a Neural Network Based PID Controller*, Sensors, vol. 17, no. 8, p. 1865 (2017), DOI: 10.3390/s17081865.

[25] Almeshal A.M., Alenezi M.R., *A Vision-Based Neural Network Controller for the Autonomous Landing of a Quadrotor on Moving Targets*, Robotics, vol. 7, no. 4, p. 71 (2018), DOI: 10.3390/robotics7040071.

[26] Levine W.S., Ed., *The Control Handbook*, CRC Press, Inc., Ashwin J. Shah, Jaico Publishing House, 121, M.G. Road, Mumbai – 400 023 (1999).

[27] Urbanski K., Zawirski K., *Improved Method for Position Estimation Using a Two-Dimensional Scheduling Array*, Automatika – Journal for Control, Measurement, Electronics, Computing and Communications, vol. 56, no. 3, pp. 331–340 (2015), DOI: 10.7305/automatika.2015.12.732.

[28] PL-Grid Infrastructure – Welcome – Infrastruktura PL-Grid: www.plgrid.pl/en.